

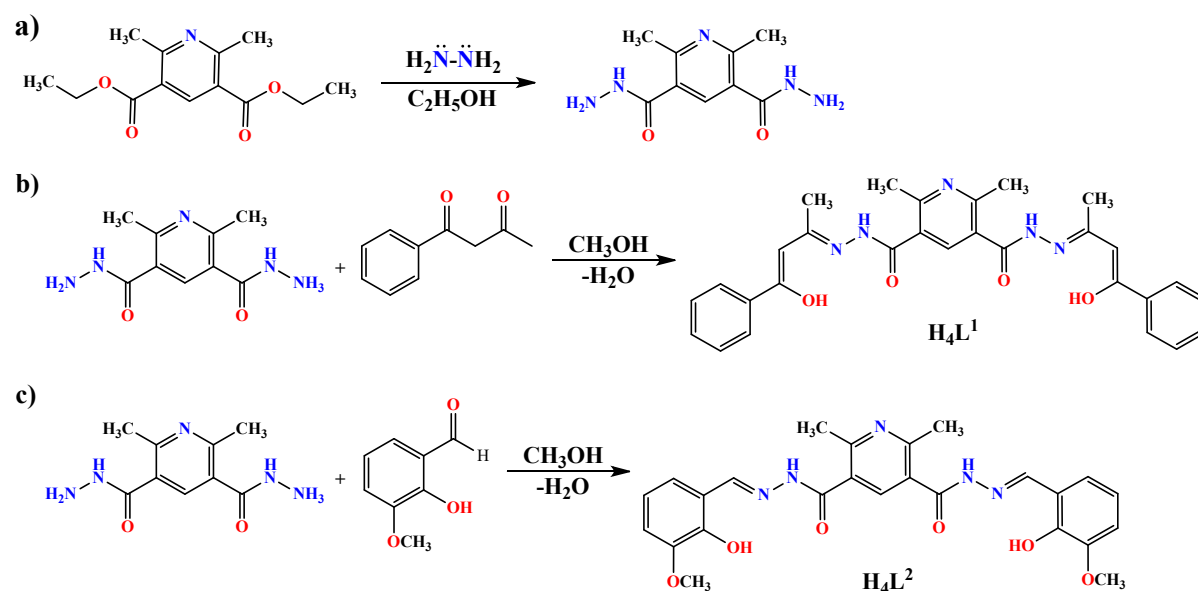
Dincular oxidovanadium complexes with dihydrazone ligands derived from diethyl 2,6-dimethylpyridine-3,5-dicarboxylate obtained from Hantzsch reaction; crystal structure and catalytic activity

Fatemeh Soltani,^a Rahman Bikas,^{a,*} Neda Heydari,^b Anna Kozakiewicz-Piekarz^c

^a Department of Chemistry, Faculty of Science, Imam Khomeini International University, 34148-96818, Qazvin, Iran

^b Department of Chemistry, Faculty of Science, University of Zanjan, 45371-38791, Zanjan, Iran

^c Department of Biomedical and Polymer Chemistry, Faculty of Chemistry, Nicolaus Copernicus University in Torun, 87-100, Torun, Poland



Scheme S1. Synthesis pathway of a) dihydrazone compound, b) H_4L^1 and c) H_4L^2

Table S1. Hydrogen bonding interactions for **1** and **2** (Å, °)

D–H···A	D–H	H···A	D···A	D–H···A
Complex 1				
C15–H15C···N11 ⁱⁱ	0.98	2.62	3.488(6)	148
O24A–H24A···O21 ⁱⁱⁱ	0.84	2.02	2.840(14)	167
O24A–H24A···N25 ⁱⁱⁱ	0.84	2.49	2.964(12)	117
N25–H25A···O21 ^{iv}	0.87	2.29	3.088(6)	152
N25–H25A···O22 ^{iv}	0.87	2.36	3.080(5)	141
N25–H25B···O1W	0.89	2.06	2.948(7)	175
N25–H25C···O21	0.88	1.91	2.781(5)	173
N25–H25D···O22 ^v	0.87	1.98	2.833(5)	166
N25–H25D···O24B ^v	0.87	2.36	2.824(15)	114
O1W–H1WA···N19 ^{vi}	0.94	1.78	2.720(15)	180
Complex 2				
C6A–H6A···O21A ⁱ	0.98	2.65	3.133(6)	110
C6A–H6C···O22B ⁱⁱ	0.98	2.61	3.573(6)	168
C6B–H6F···O21B ⁱⁱⁱ	0.98	2.65	3.288(6)	123
O1W–H1WA···O14B ^{iv}	0.86	2.28	3.091(5)	158
O1W–H1WB···N18A	0.86	2.02	2.841(5)	161
N24–H24A···O21A	0.99	1.86	2.827(5)	163
N24–H24B···O1W ^v	0.99	1.95	2.909(5)	161
N24–H24C···O22A ^{vi}	0.99	1.83	2.829(5)	175
N24–H24D···O5B ⁱ	0.99	2.34	2.966(5)	120
N24–H24D···O8B ⁱ	0.99	1.99	2.967(5)	166
N23–H23A···O22B ^{vii}	0.99	1.88	2.867(5)	166
N23–H23B···O1W ^{iv}	0.99	2.16	3.100(5)	156
N23–H23C···O22A ⁱⁱⁱ	0.99	2.34	2.990(5)	122
N23–H23C···O21B	0.99	2.04	2.765(5)	128
N23–H23D···O5A ⁱⁱⁱ	0.99	2.08	2.890(5)	137
N23–H23D···O8A ⁱⁱⁱ	0.99	2.07	2.931(5)	144

Symmetry codes: for **1** (ii) $x, -y+1, z-1/2$; (iii) $x, y, z-1$; (iv) $x, -y+2, z+1/2$; (v) $x, y, z+1$; (vi) $-x+1, -y+1, -z+2$; for **2** (i) $-x+1, y-1/2, -z+3/2$; (ii) $x, y-1, z$; (iii) $-x+2, y+1/2, -z+3/2$; (iv) $-x+2, -y+1, -z+1$; (v) $-x+1, -y+1, -z+1$; (vi) $x-1, y, z$; (vii) $x+1, y, z$.

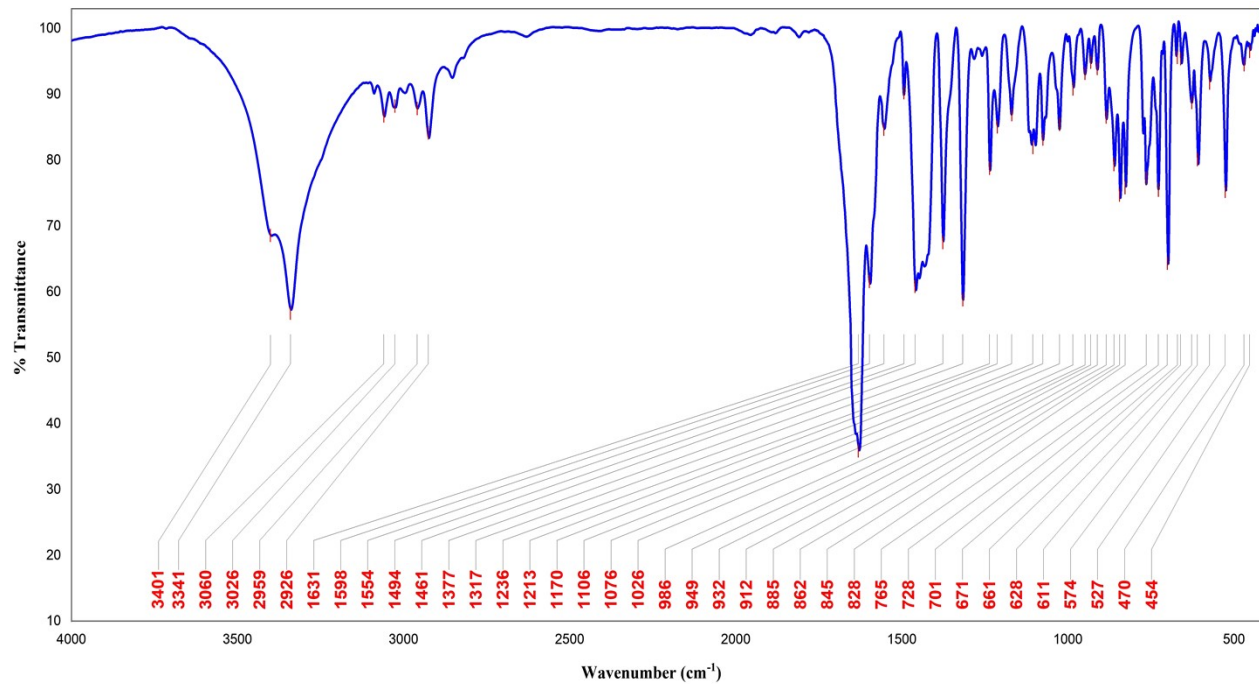


Fig. S1. FT-IR spectrum of H₄L¹

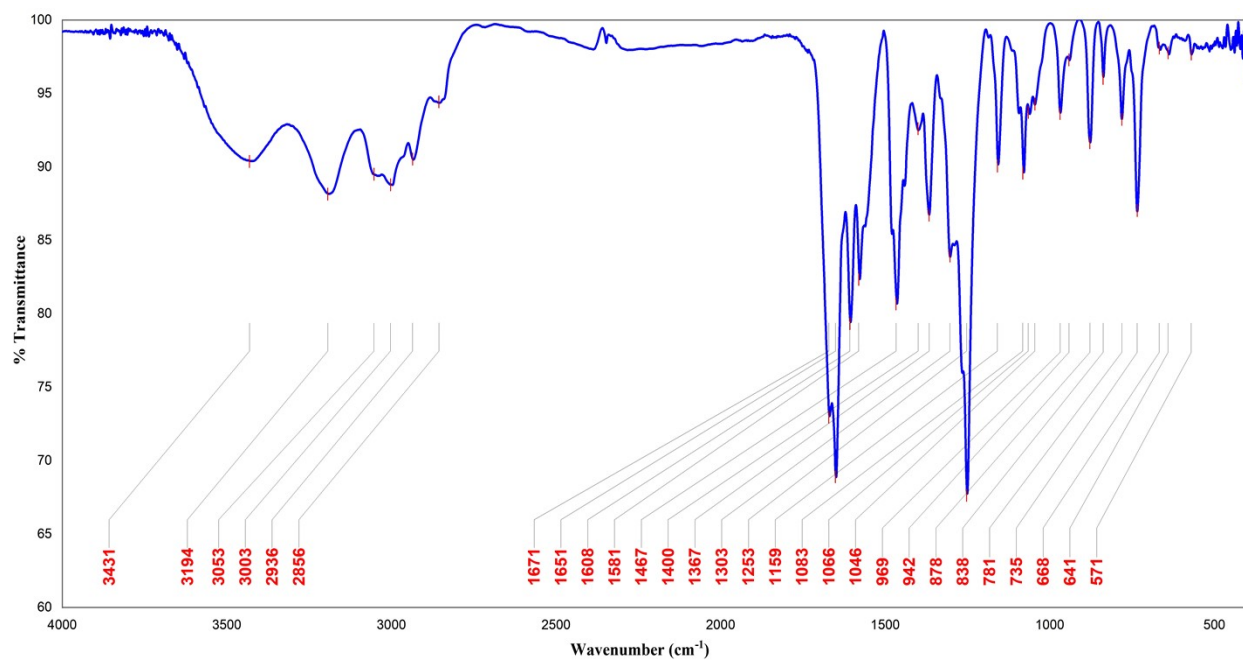


Fig. S2. FT-IR spectrum of H₄L²

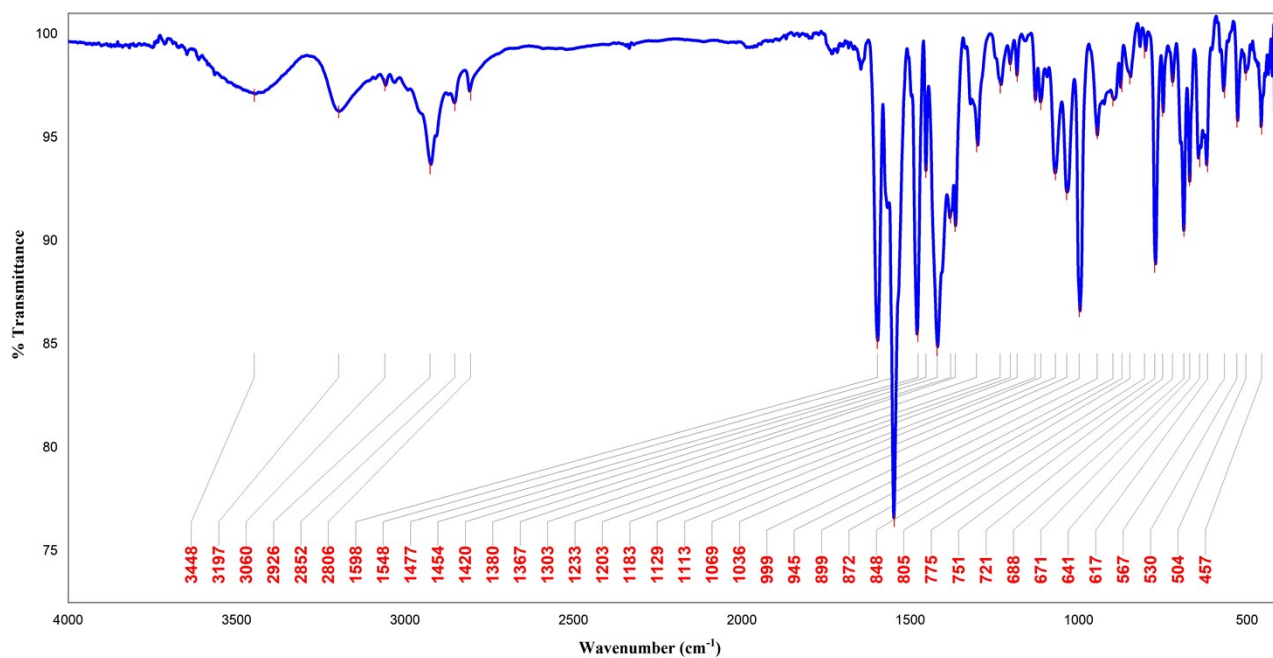


Fig. S3. FT-IR spectrum of compound 1

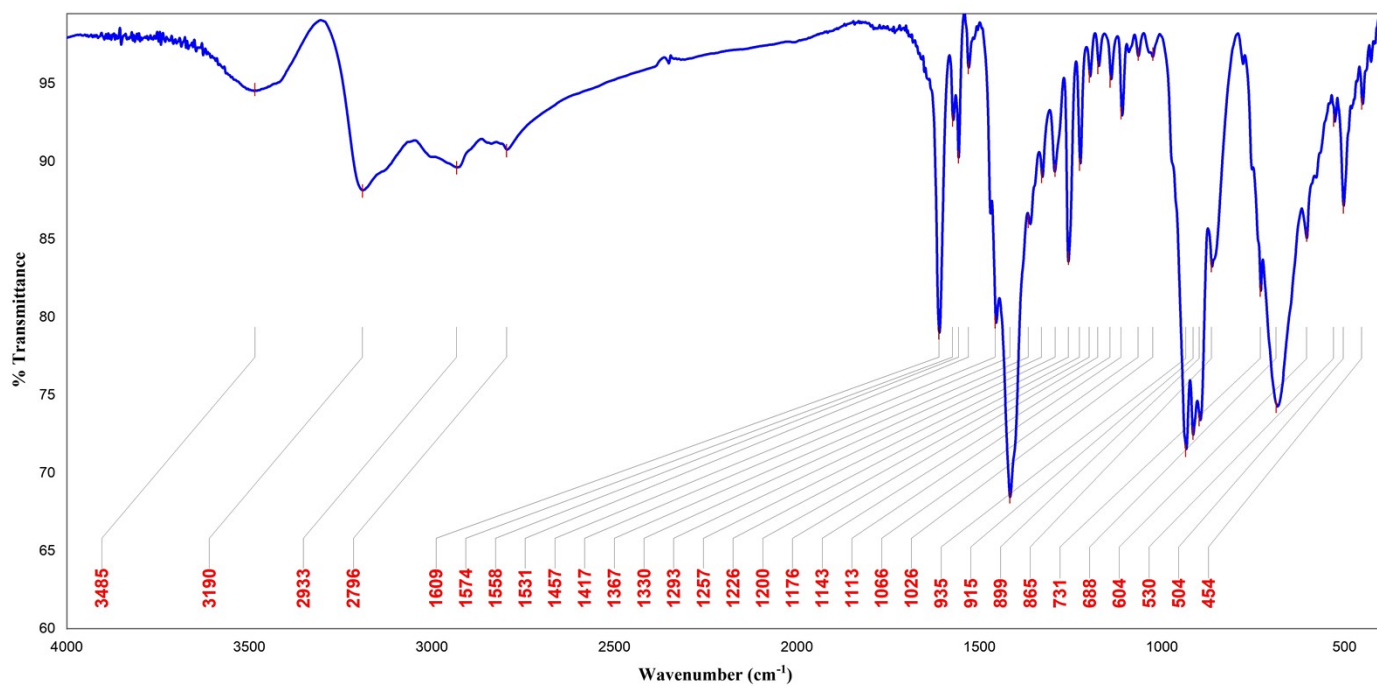


Fig. S4. FT-IR spectrum of compound 2

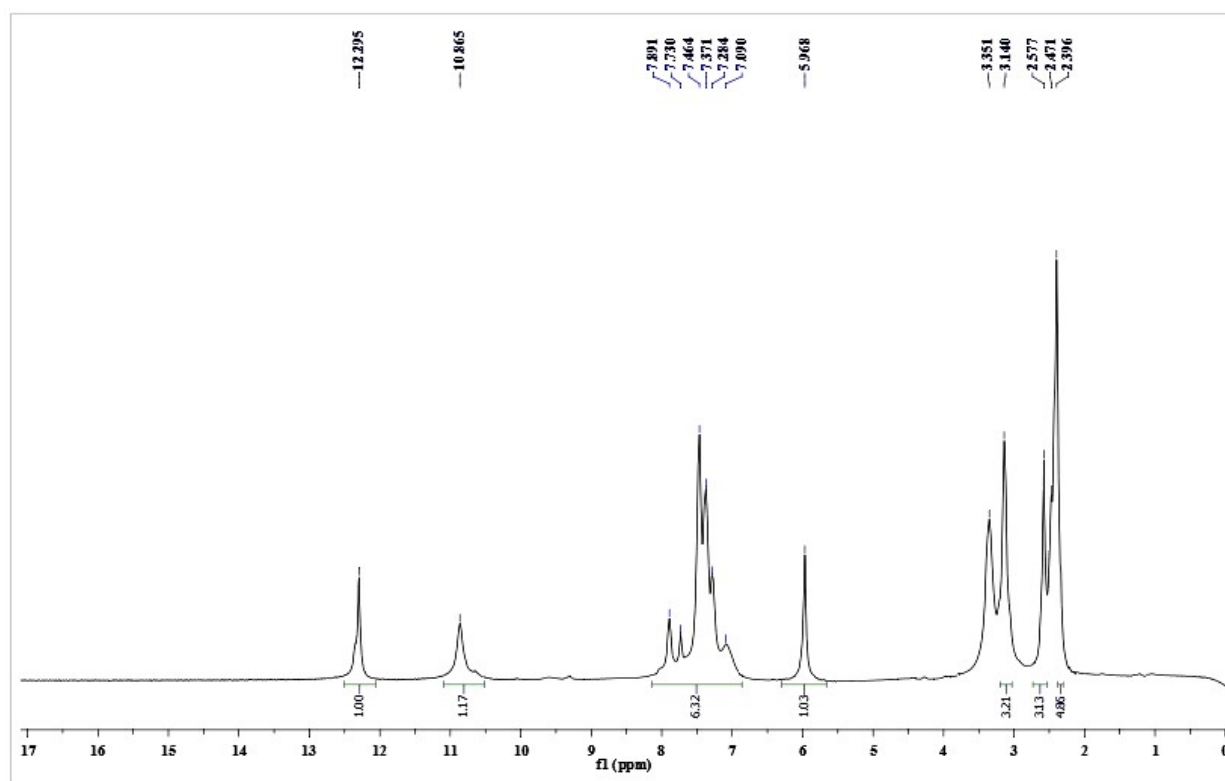


Fig. S5. ^1H NMR spectrum of H_4L^1 in DMSO-d_6

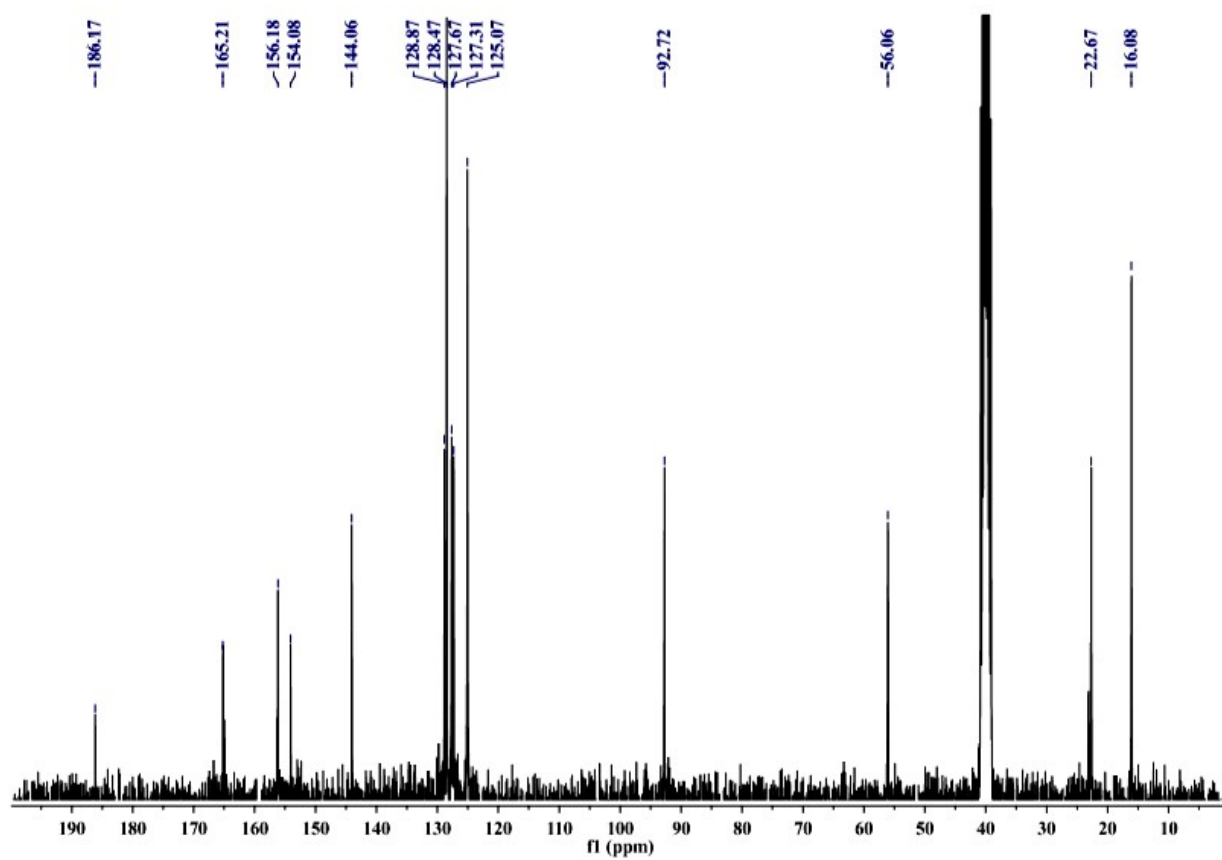


Fig. S6. ^{13}C NMR spectrum of H_4L^1 in DMSO-d_6

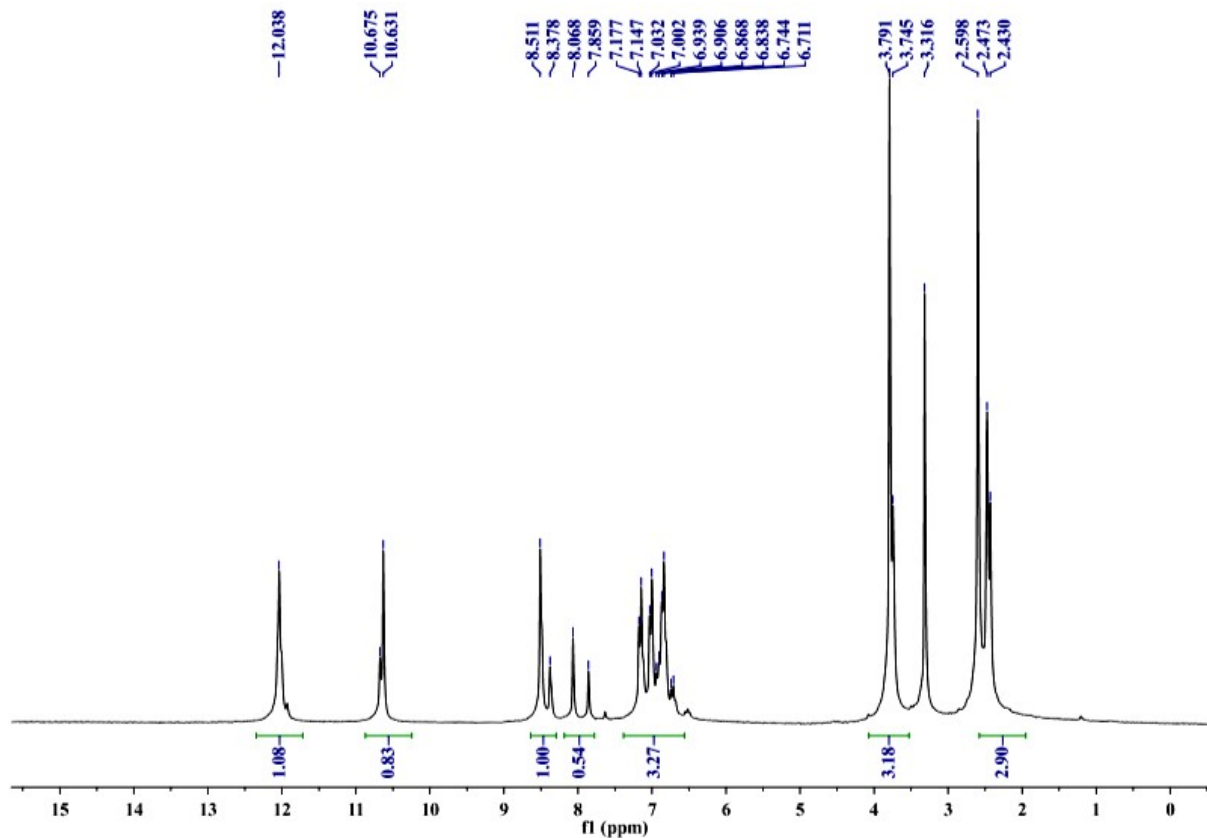


Fig. S7. ^1H NMR spectrum of H_4L^2 in DMSO-d_6

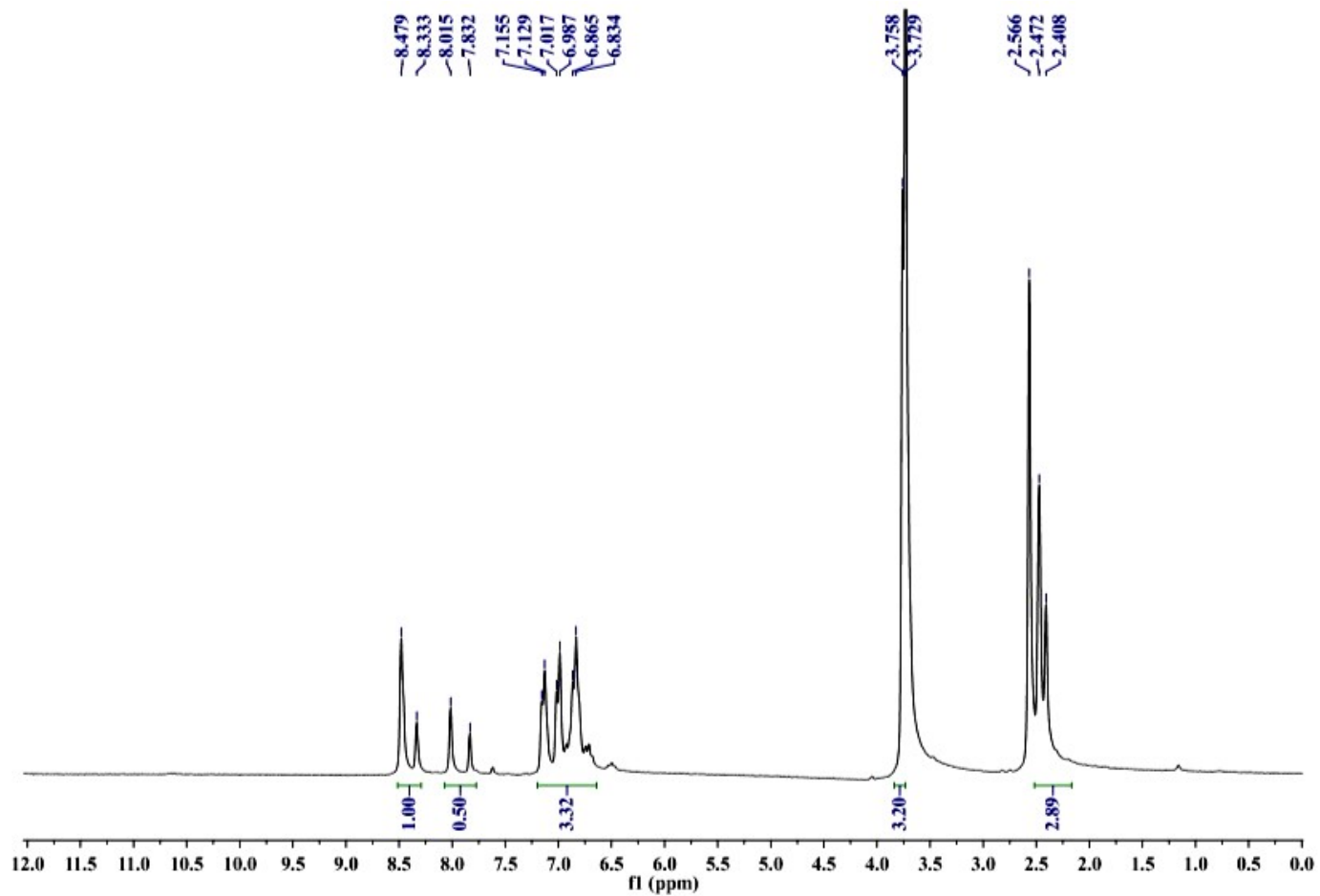


Fig. S8. ^1H NMR spectrum of H_4L^2 in $\text{DMSO-d}_6 + \text{D}_2\text{O}$

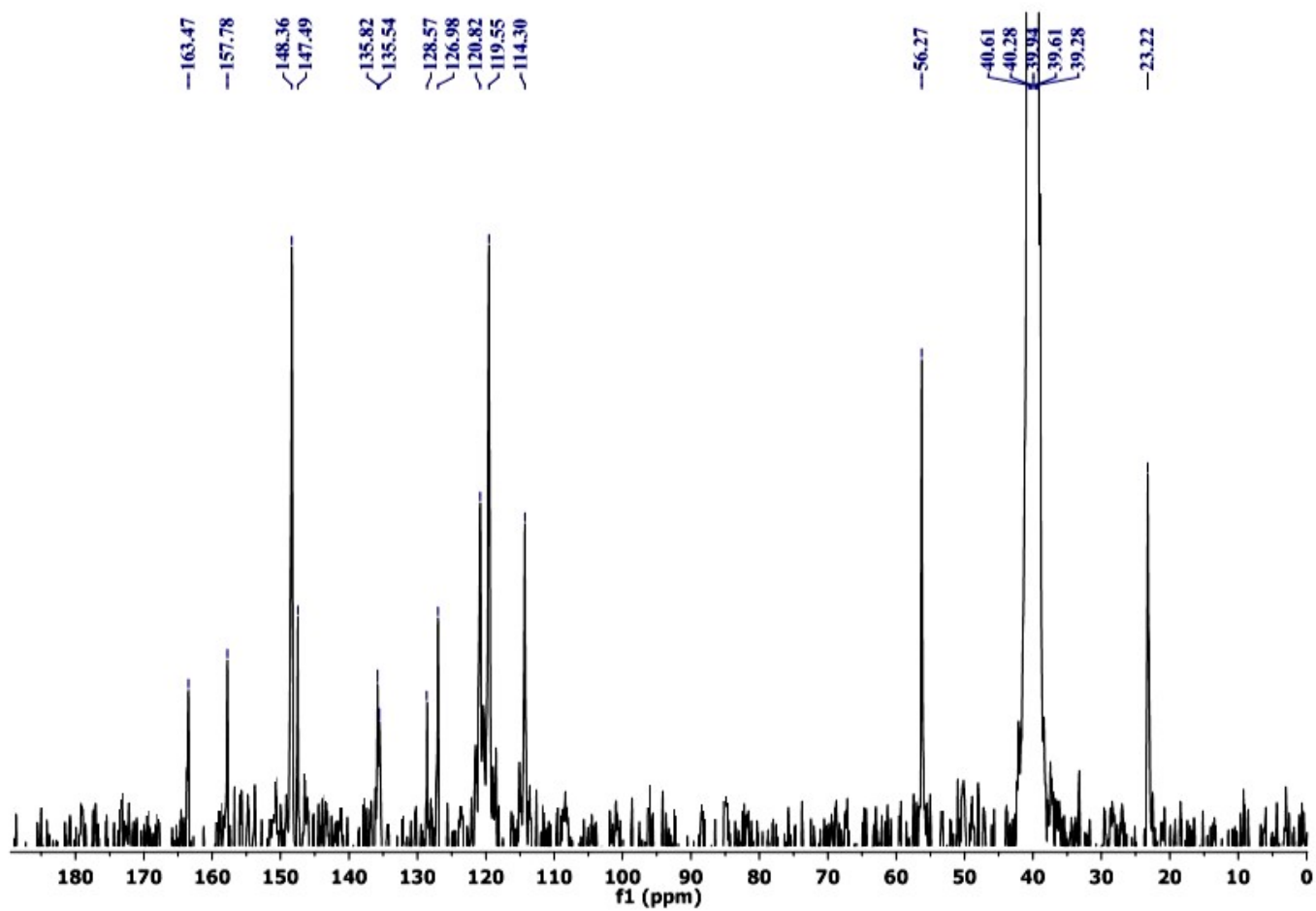


Fig. S9. ^{13}C NMR spectrum of H_4L^2 in DMSO-d_6

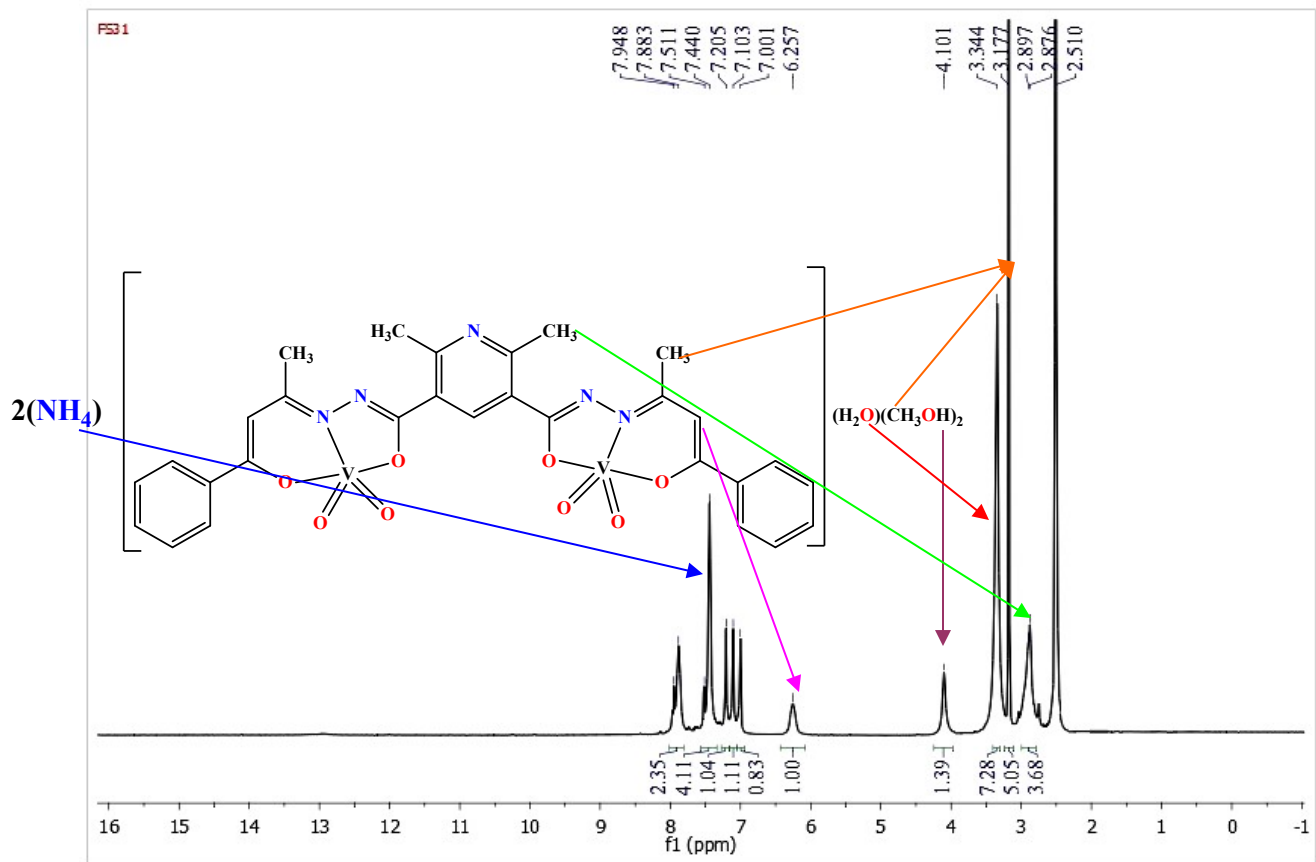


Fig. S10. ¹H NMR spectrum of complex **1** in DMSO-d₆

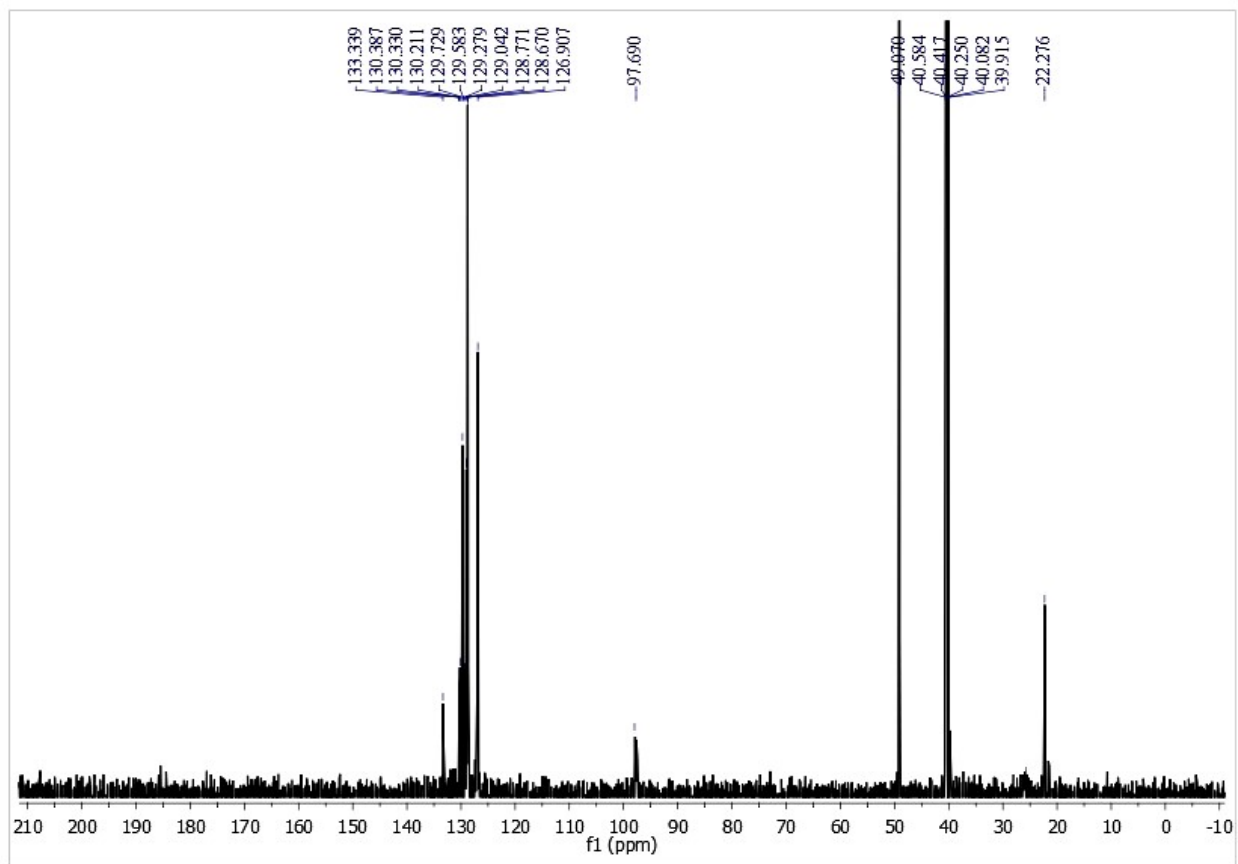


Fig. S11. ^{13}C NMR spectrum of complex **1** in DMSO-d_6

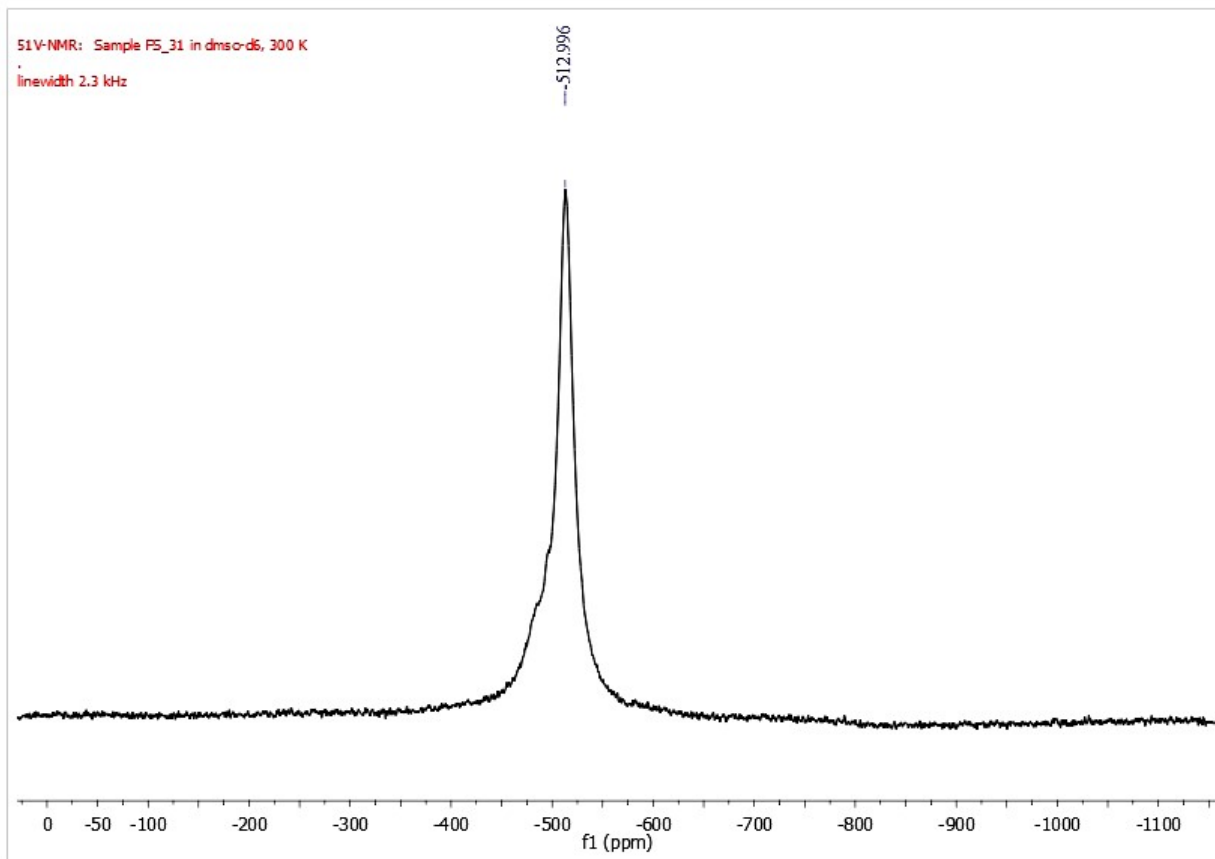


Fig. S12. ^{51}V NMR spectrum of complex **1** in DMSO- d_6

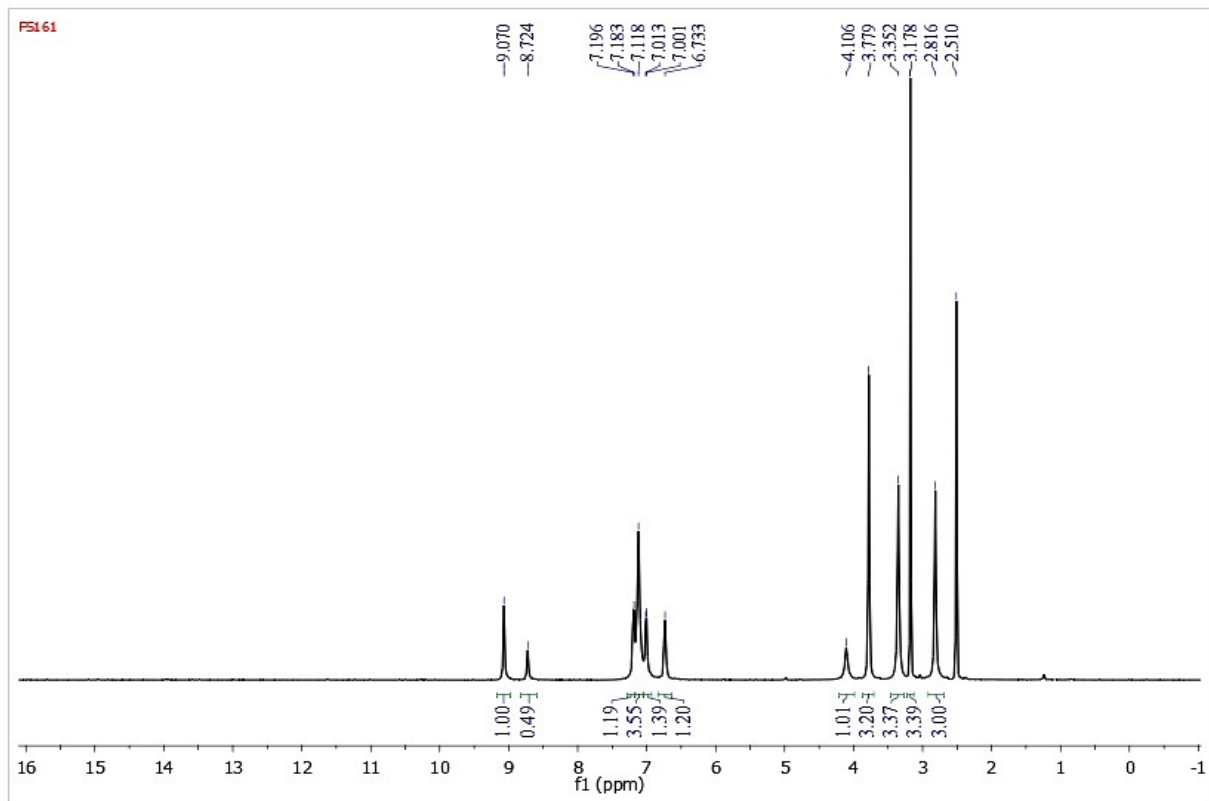


Fig. S13. ^1H NMR spectrum of complex **2** in DMSO-d_6 (300 MHz)

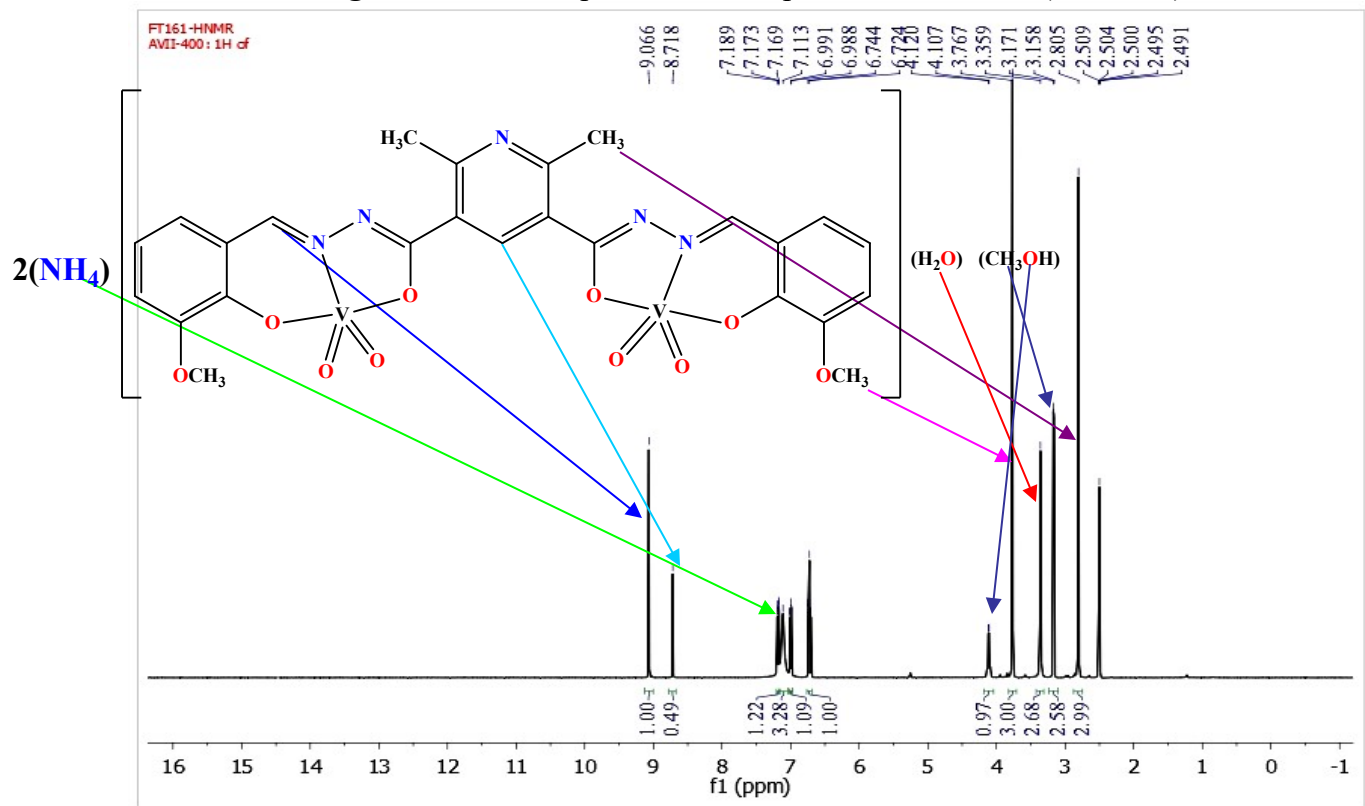


Fig. S14. ^1H NMR spectrum of complex **2** in DMSO-d_6 (400 MHz)

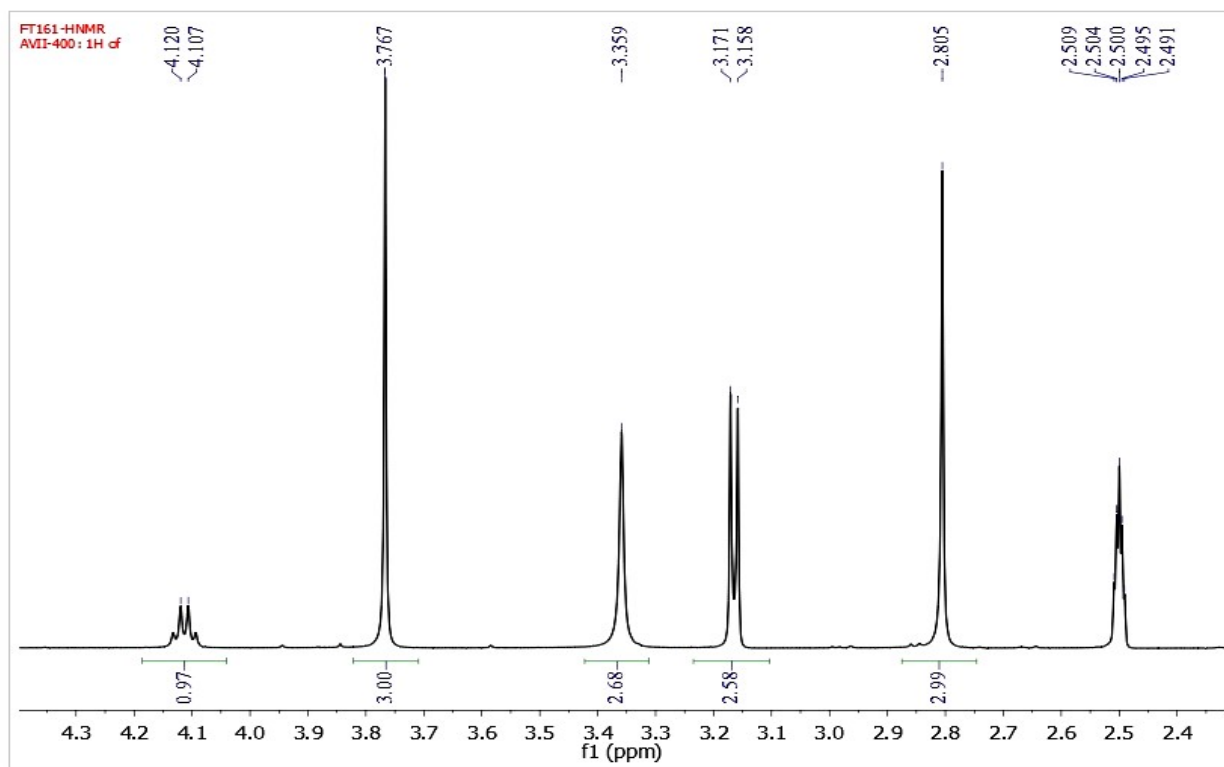
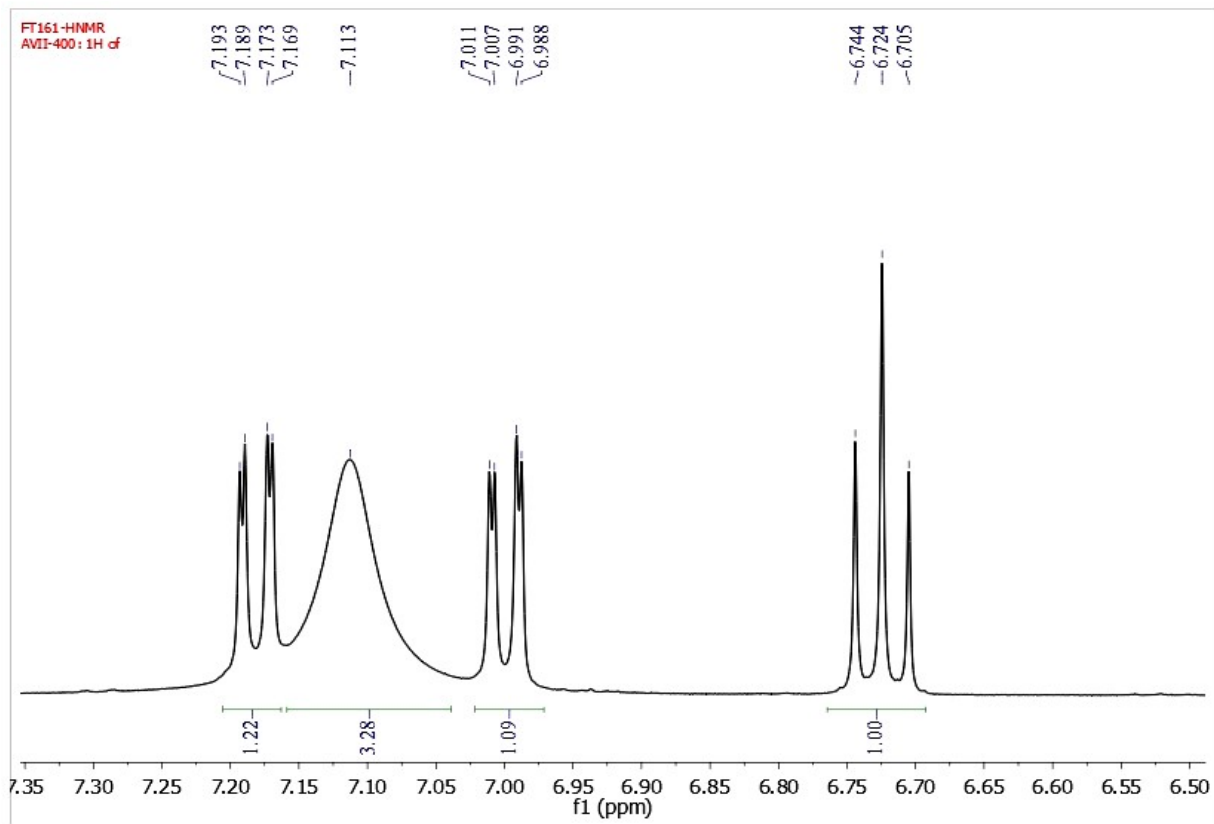


Fig. S15. Expanded ^1H NMR spectrum of complex **2** in DMSO-d_6 (top 6.5-7.5 ppm; bottom 2.3-4.3 ppm)

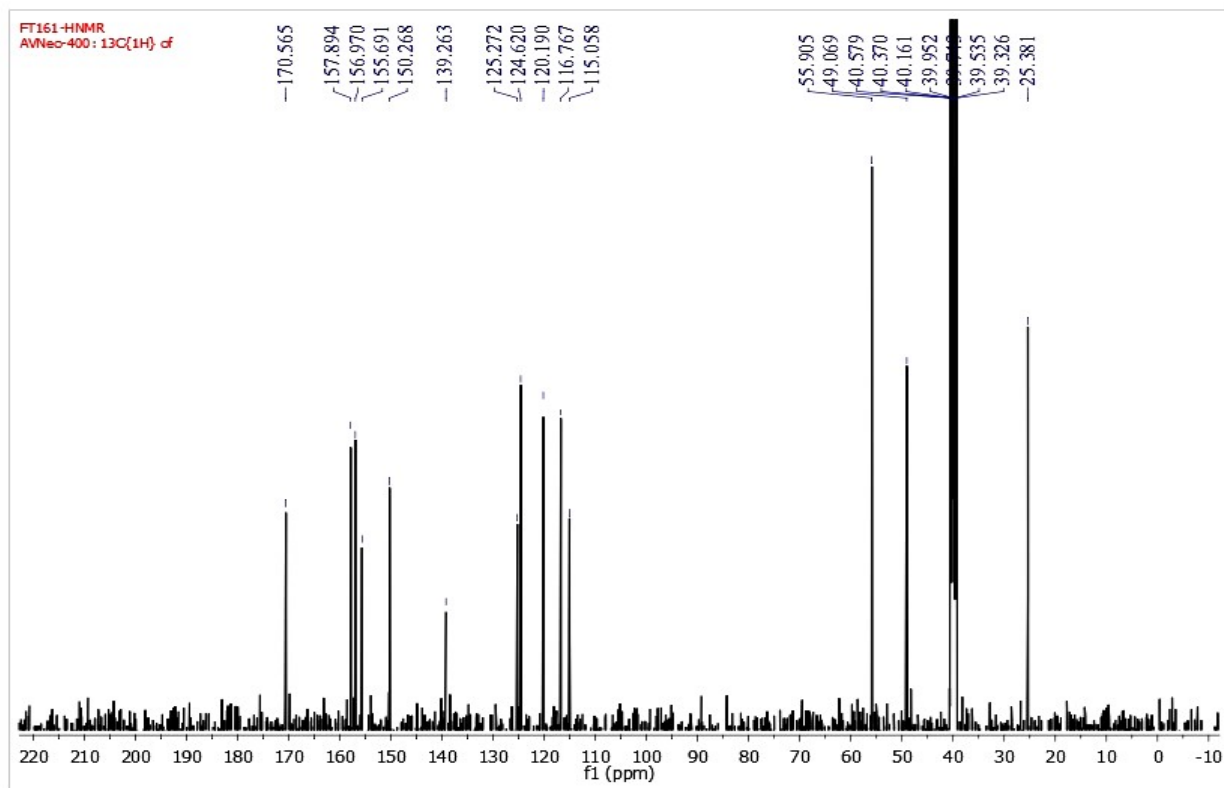


Fig. S16. ^{13}C NMR spectrum of complex **2** in DMSO-d_6

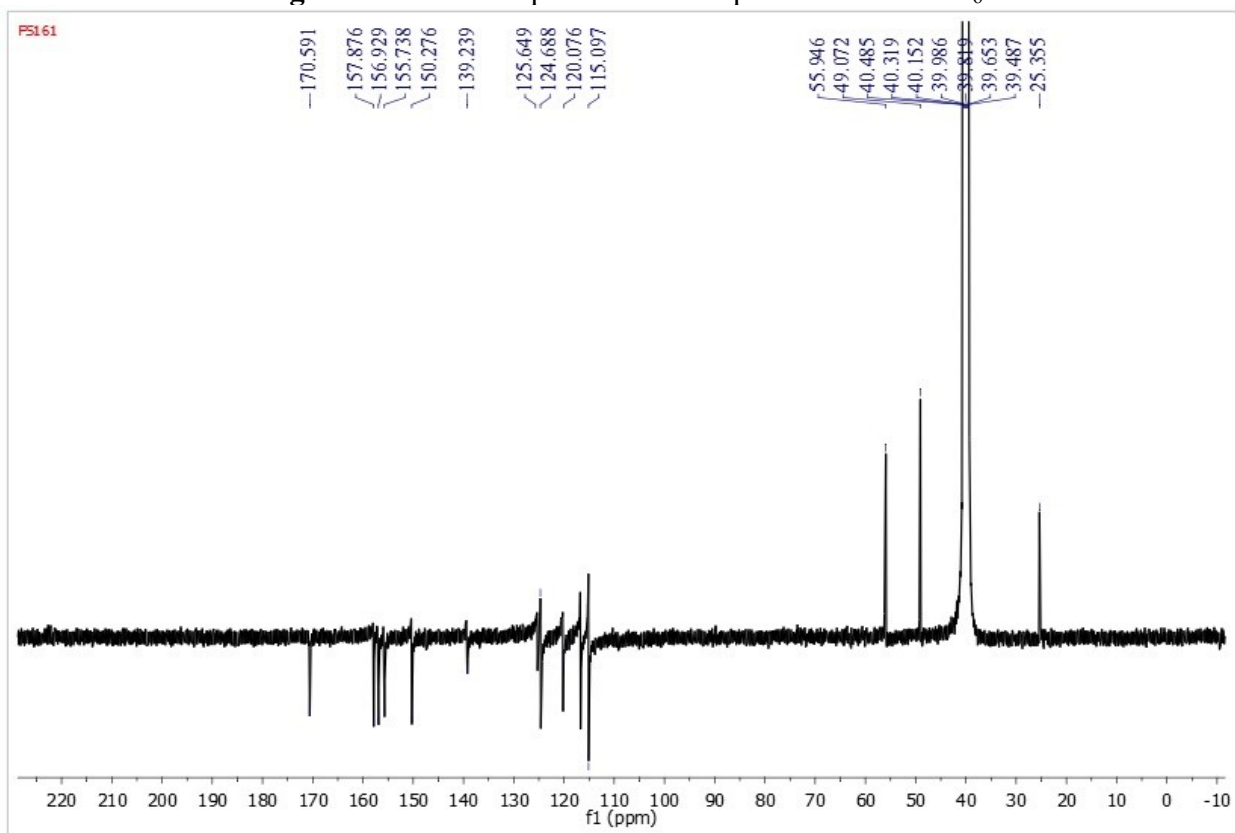


Fig. S17. DEPT ^{13}C NMR spectrum of complex **2** in DMSO-d_6

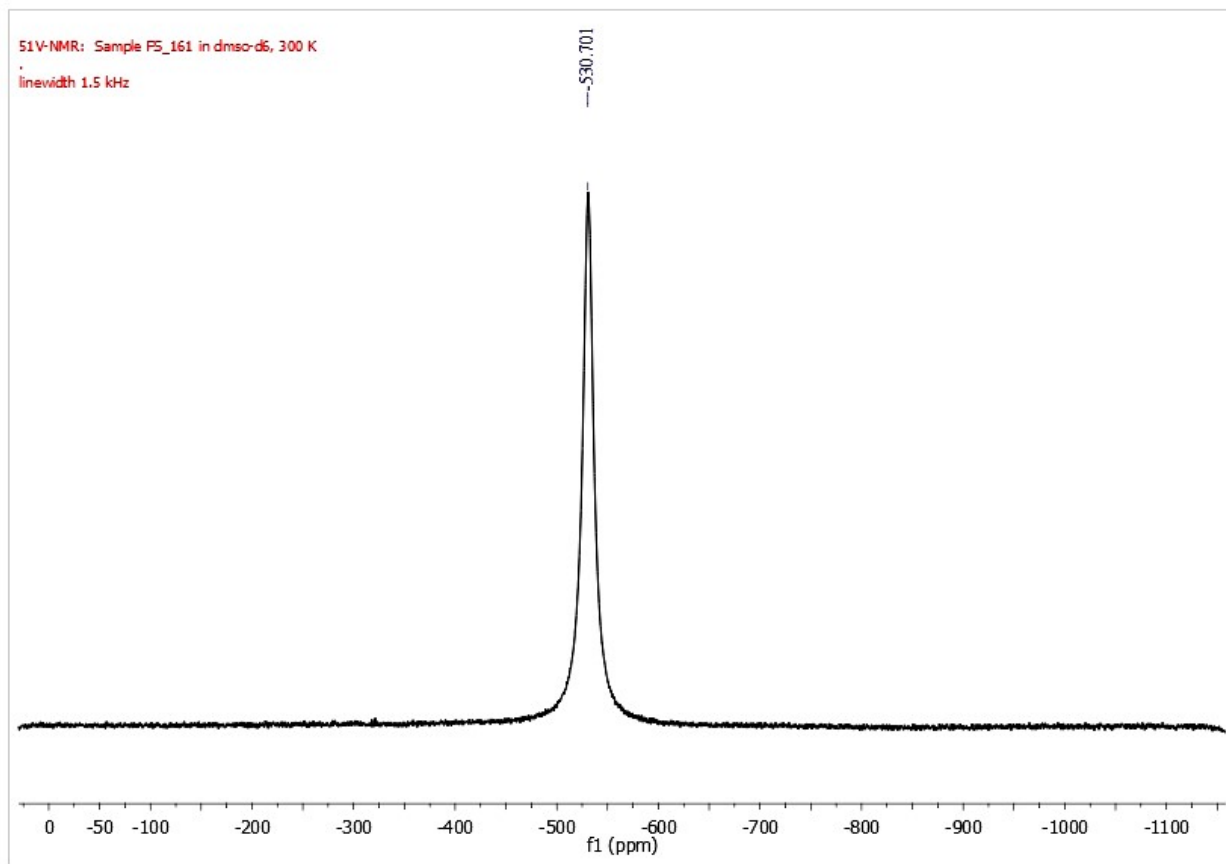


Fig. S18. ^{51}V NMR spectrum of complex **2** in DMSO-d_6

Line#:1 R.Time:----(Scan#----)
MassPeaks:167
RawMode:Averaged 0.333-0.640(201-385) BasePeak:159.15(328188)
BG Mode:Averaged 0.700-0.973(421-585) Segment 1 - Event 1

FS31

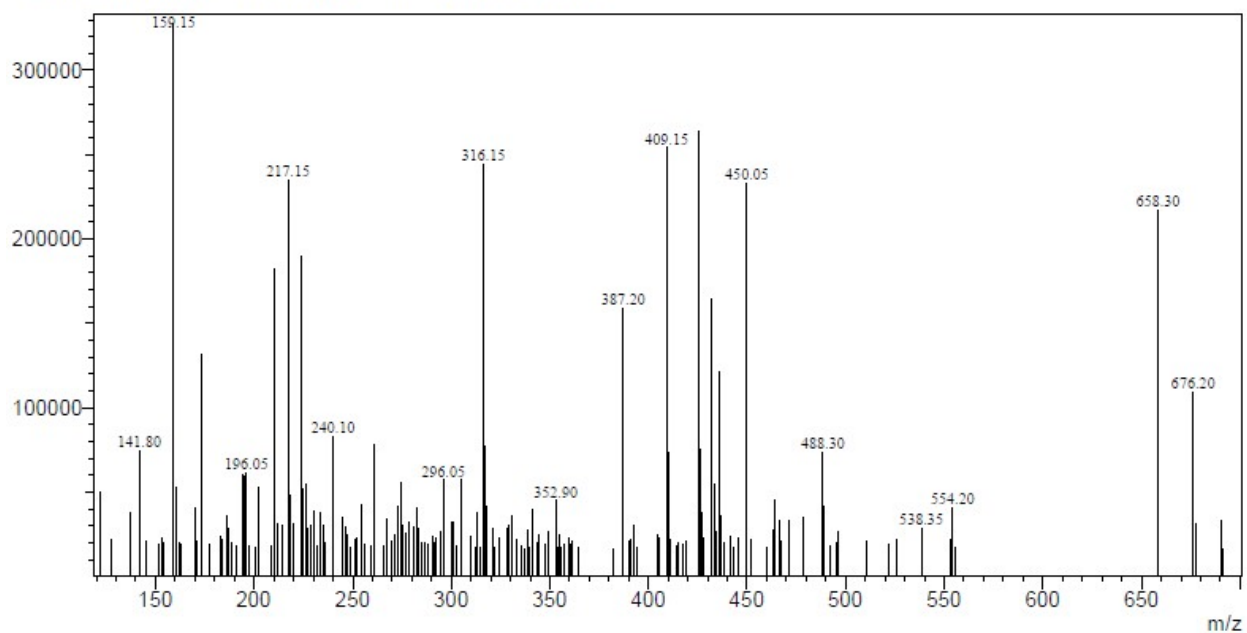


Fig. S19. Mass spectrum of complex 1

Line#:1 R.Time:0.580(Scan#:349)
MassPeaks:22
RawMode:Single 0.580(349) BasePeak:453.10(20000000)
BG Mode:None Segment 1 - Event 1

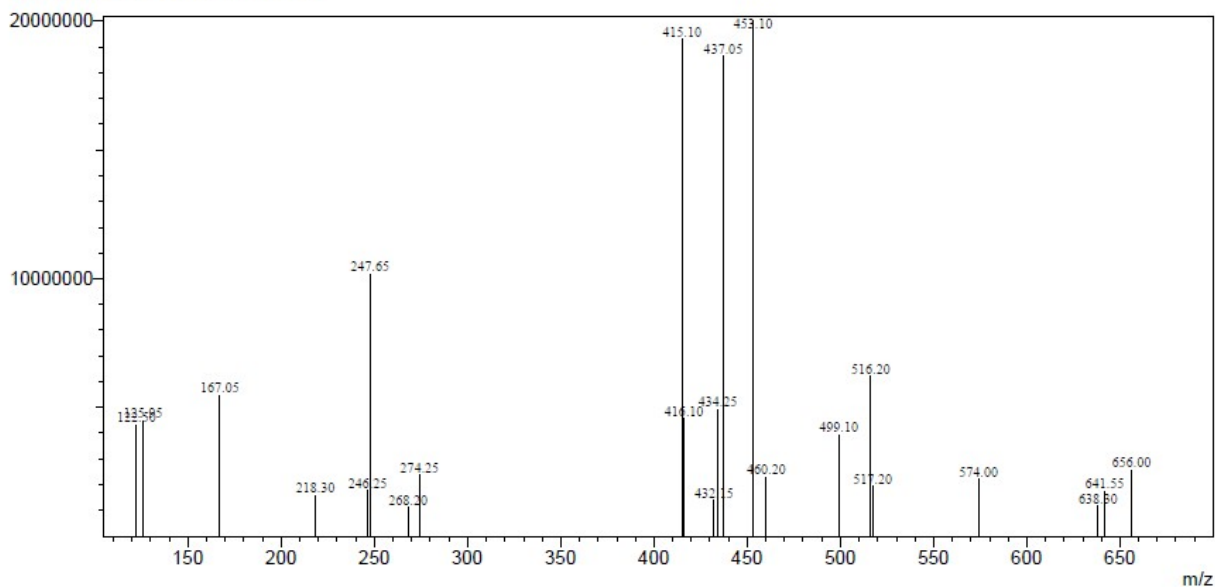


Fig. S20. Mass spectrum of complex 2

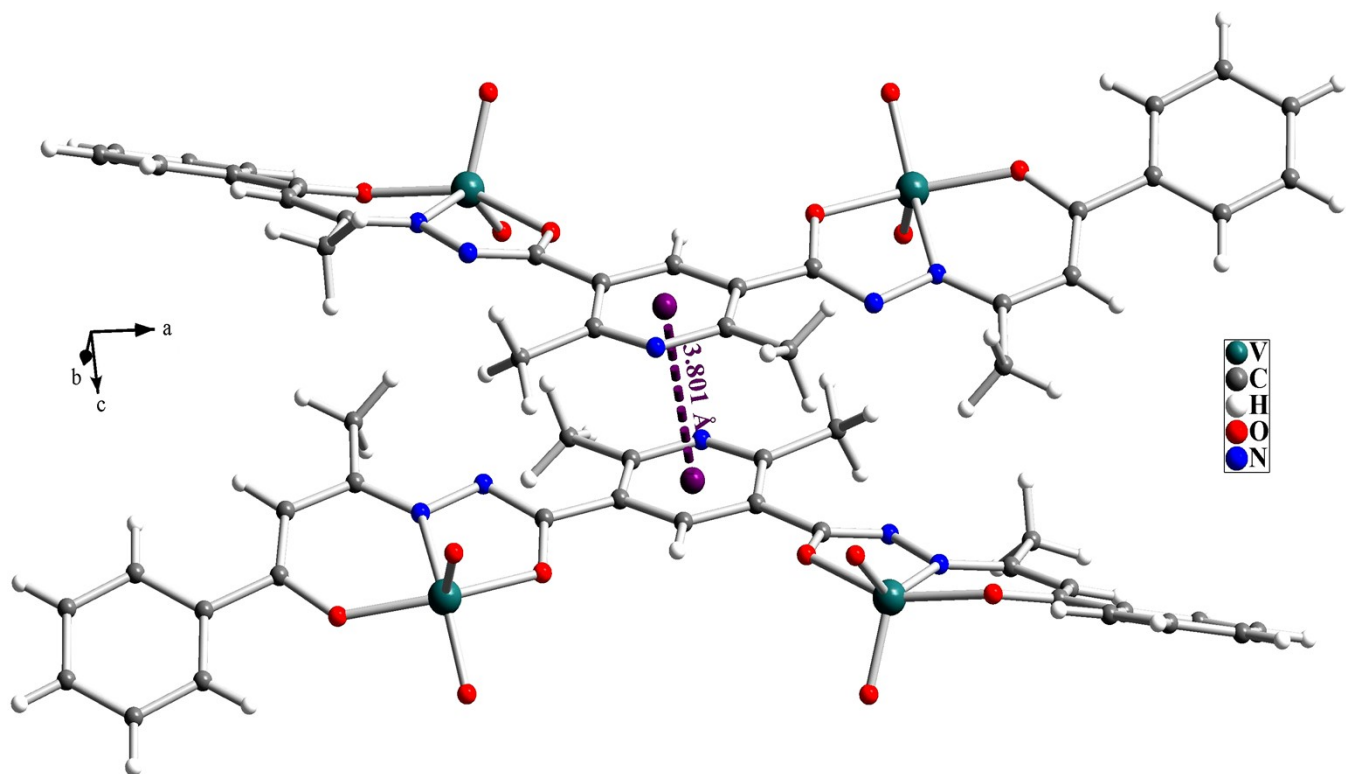


Fig. S21. Intermolecular $\pi \cdots \pi$ stacking interaction in the crystal structure of complex 1

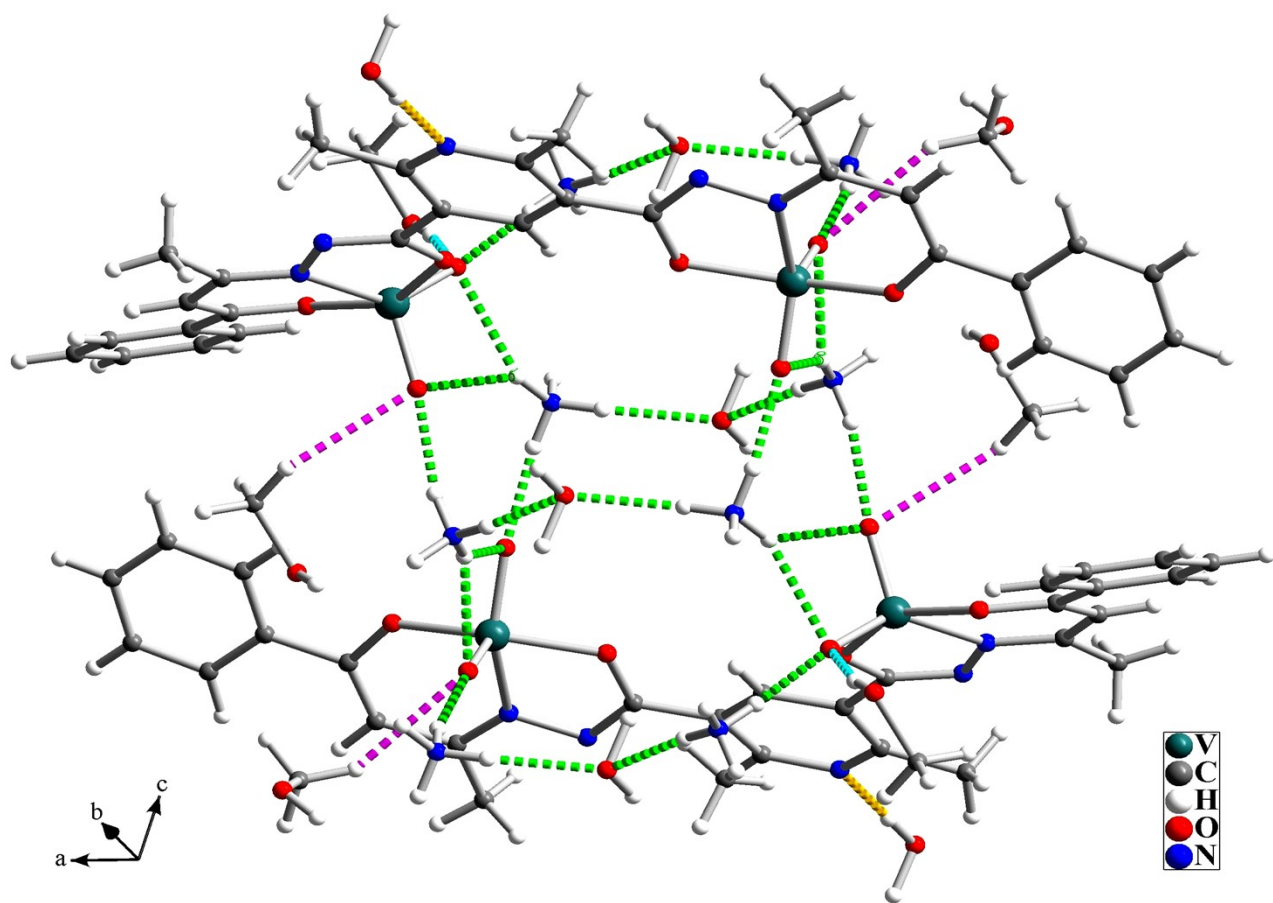


Fig. S22. Hydrogen bond interactions in the crystal structure of complex **1**; O–H...N (orange), O–H...O (blue), N–H...O (green) and C–H...O (pink)

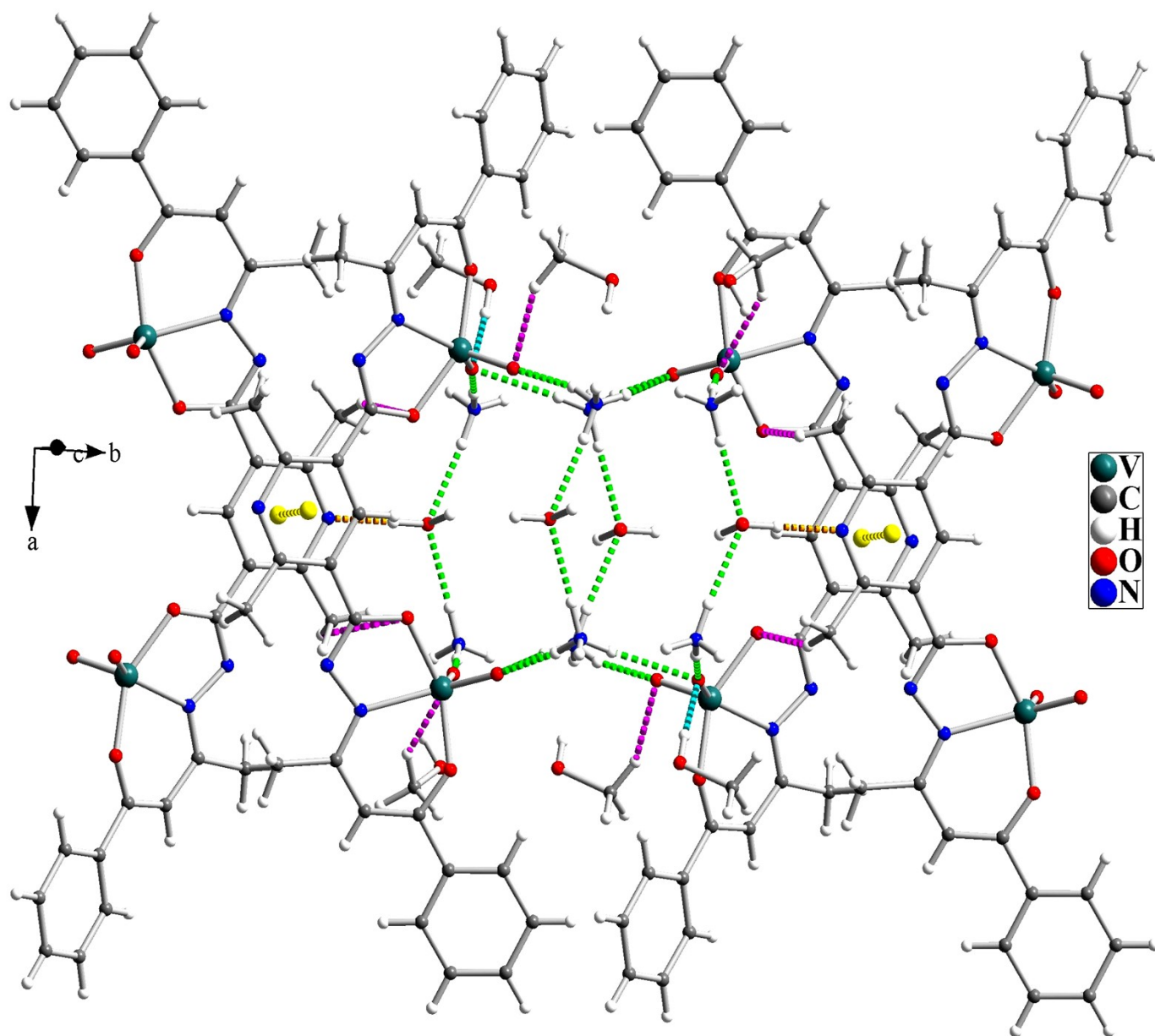


Fig. S23. Intermolecular $\pi \cdots \pi$ stacking (yellow dashed line) and $\text{O-H} \cdots \text{N}$ (orange), $\text{O-H} \cdots \text{O}$ (blue), $\text{N-H} \cdots \text{O}$ (green) and $\text{C-H} \cdots \text{O}$ (pink) hydrogen bond interactions in the crystal structure of complex 1

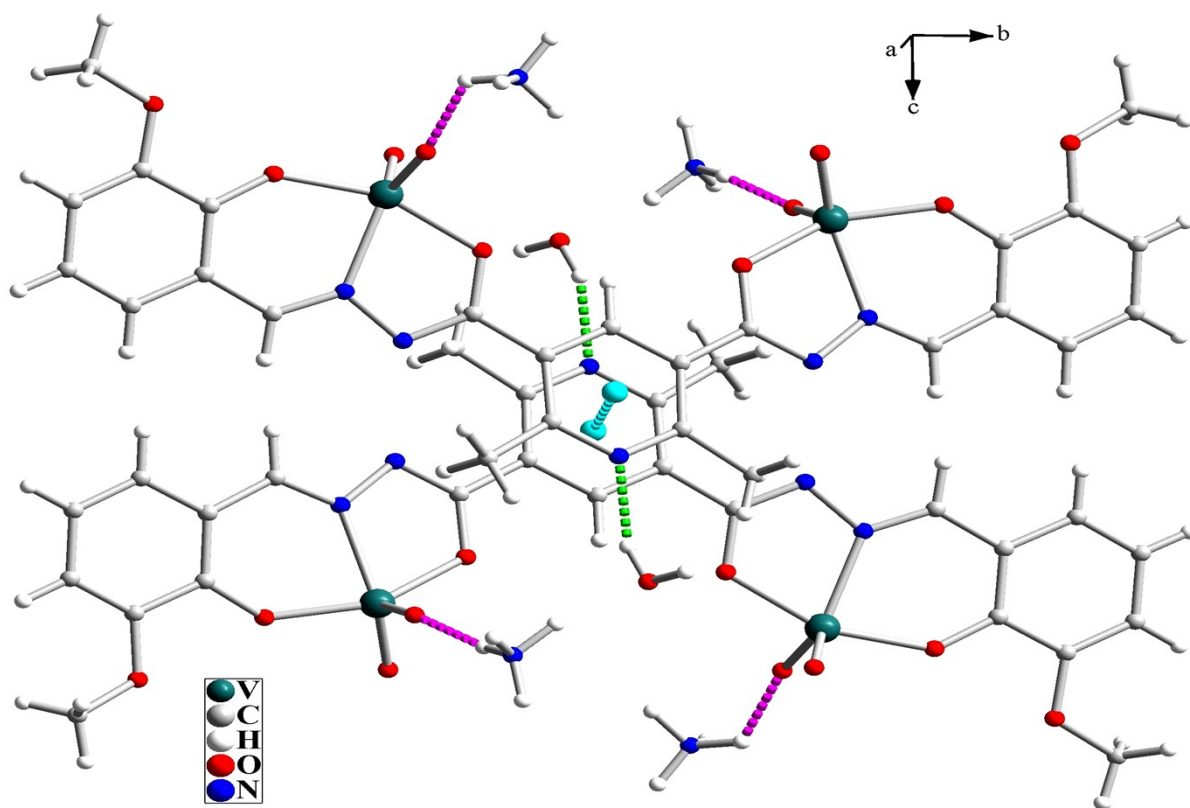


Fig. S24. Intermolecular $\pi\cdots\pi$ stacking (blue dashed line) and hydrogen bond interactions O–H \cdots N (green) and N–H \cdots O (pink) in the crystal structure of complex **2**

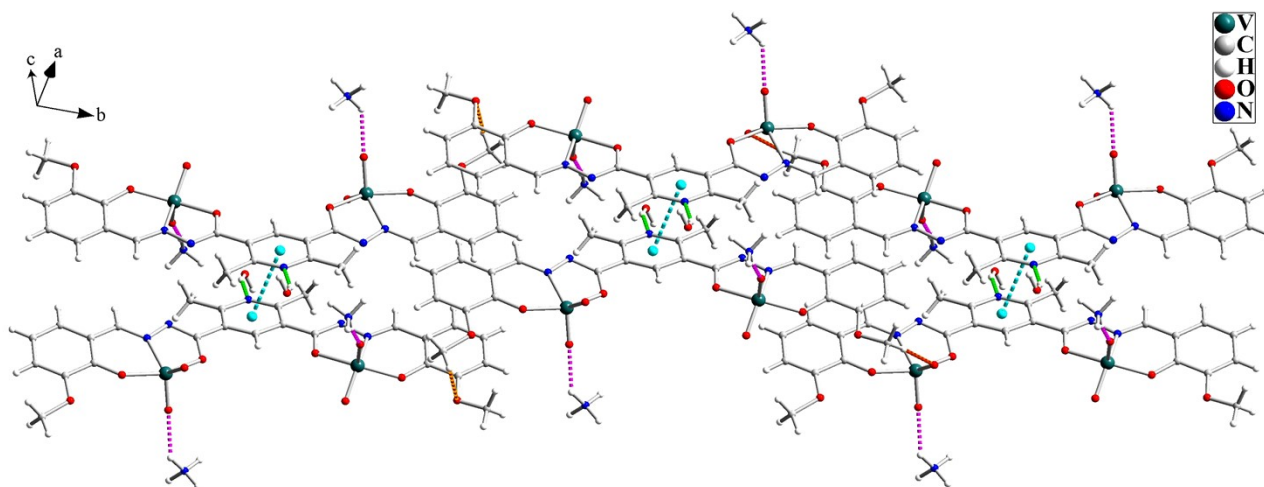


Fig. S25. Intermolecular $\pi\cdots\pi$ stacking (blue dashed line) and O–H \cdots N (green), N–H \cdots O (pink) and C–H \cdots O (orange) hydrogen bond interactions in the crystal structure of complex **2**

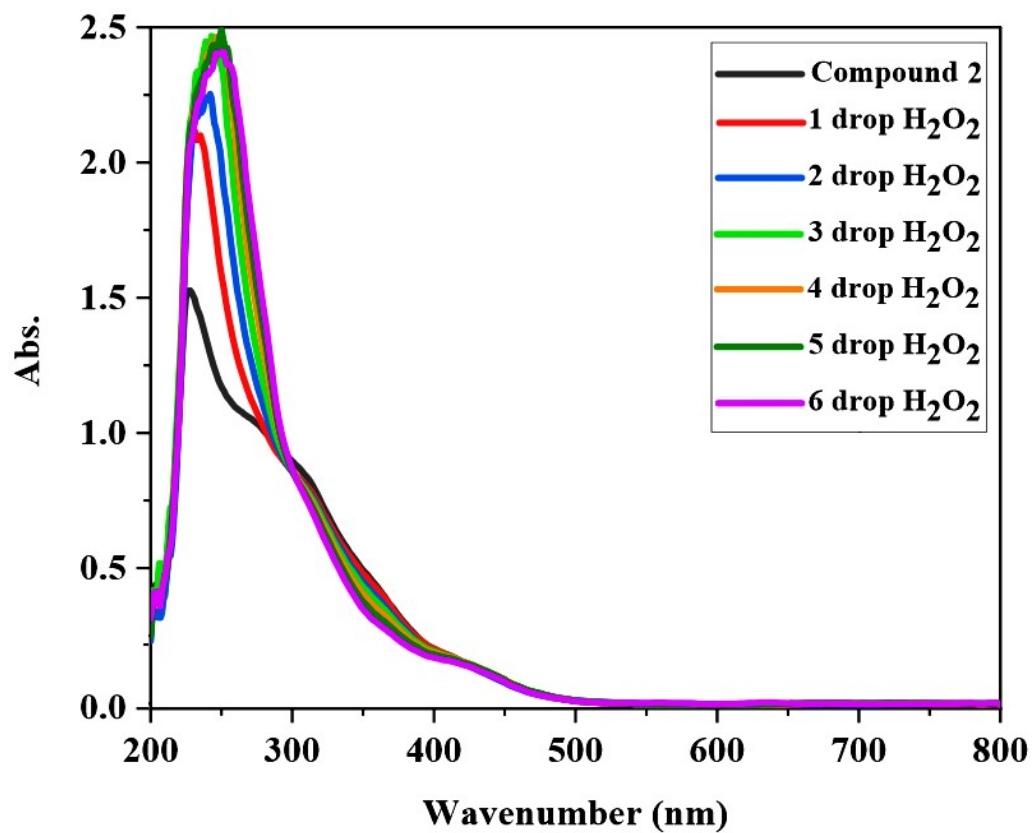


Fig. S26. UV-Vis spectra of complex 2 after addition of diluted H₂O₂ in CH₃OH